Convection in a horizontal fluid layer under an inclined temperature gradient

A. S. Ortiz-Pérez and L. A. Dávalos-Orozco
Instituto de Investigaciones en Materiales, Departamento de Polímeros, Universidad Nacional Autónoma de México, Ciudad Universitaria, Circuito Exterior S/N, Delegación Coyoacán, 04510 México D. F., México

(Received 26 August 2010; accepted 25 July 2011; published online 19 August 2011)

In this paper, we investigate the flow instability of a horizontal fluid layer under an inclined temperature gradient. The fluid layer is supposed to be of infinite extension, and the differentially heated lateral walls are very far away from the central region which is the subject of research. The layer is also inside two rigid, horizontal and parallel walls which are perpendicular to gravity and subjected to a vertical adverse temperature gradient. Calculations are done for Prandtl numbers Pr in the range from 0.026 to 1, which include materials from liquid metals to gases. By improving the Galerkin numerical method, new results and important extensions and corrections to the work of Nield [Int. J. Heat Fluid Flow **15**, 157 (1994)] are obtained. It is found that inside the range $0.2 < \mathrm{Pr} < 0.45$, a new oblique oscillatory mode starts to appear and that it can be the first unstable one in a particular range of the horizontal Rayleigh number R_H for all Prandtl numbers until $\mathrm{Pr} = 1$. To the left, this mode separates from an oscillatory longitudinal even mode already found by Nield [Int. J. Heat Fluid Flow **15**, 157 (1994)]. A new codimension two point is found when the Prandtl number is increased to $\mathrm{Pr} = 0.4886$, where the curves of the oblique oscillatory mode and the even stationary longitudinal mode touch each other for the first time. Another new codimension two point starts to appear in the range $0.5 < \mathrm{Pr} < 1.0$ which corresponds to the crossing between the curves of the oblique oscillatory mode and the odd stationary longitudinal mode. As a consequence, another interesting result is that, to the right of this point, the odd stationary longitudinal mode is the first unstable one in a range of R_H. The qualitative form of the curves of criticality changes notably between $\mathrm{Pr} = 0.026$ and $\mathrm{Pr} = 1.0$. Therefore, here we present a detailed description of this change by means of calculations for different Prandtl numbers inside that range.
 [doi:10.1063/1.3626009]

I. INTRODUCTION

The problem of natural convection has been investigated since many years ago due to its presence in many natural phenomena where temperature differences exist under gravity. However, from the point of view of applications, sometimes it is important to avoid any motion due to temperature differences. Examples are processes of crystal growth and molten metals where any motion previous to solidification can produce important inhomogeneities and striations in the resulting material. In the atmosphere and oceans, temperature gradients are the source of motion of big masses of fluid. In this case, the understanding of the response of gases and liquids to their influence is of fundamental interest to investigate the climate of the earth. The convection in a horizontal infinite fluid layer heated from below has been reviewed by Chandrasekhar.[1] In the case of parallel and rigid walls, it is shown that the critical Rayleigh number (representing the ratio of buoyancy and viscous forces) has a value of 1708. If the temperature gradient is vertical and adverse, this is the minimum magnitude necessary to destabilize an unstably stratified fluid layer. In this particular situation, the starting flow is always stationary. Other convective phenomena are due to a horizontal temperature gradient. The system is supposed to be a horizontal fluid layer of very large extension and perpendicular to gravity which has two vertical differentially heated walls. A closed basic flow is produced immediately after setting the horizontal temperature gradient because the fluid starts to move upwards at the hot vertical wall and downwards at the cold vertical wall. The result is a very large cell flow. It has been shown experimentally that this motion is unstable and that it produces oscillations which are the source of a banded distribution of solute in crystals.[2] Besides, Hurle *et al.*[2] and Hart[3] investigated the instability of this flow with a very small aspect ratio, the so called Hadley circulation. Hart[3] obtained results of the critical horizontal Rayleigh number R_{HC} for a range of Prandtl numbers Pr (the ratio of the thermal and viscous diffusivities). Gill[4] investigated the particular case of liquid metals that have a very small Prandtl number ($\mathrm{Pr} = 0.026$ for mercury). Hart[5] shows that, when the horizontal walls are insulated, in a range of small Prandtl numbers, the convection is first oscillatory. Walton[6] studies the stability of a flow under a horizontal temperature gradient due to a hot-patch. Kuo *et al.*[7] present important corrections to previous work using a pseudospectral method with Chebyshev polynomials. In other papers, Kuo and Korpela [8] and Wang and Korpela[9] investigated the non linear problem for particular ranges of the Prandtl number, including good and bad conducting walls. Laure[10] and Laure and Roux[11] made numerical calculations which confirm and correct previous results in the literature. More recently, Braunsfurth *et al.*,[12] Juel *et al.*,[13] and Hof *et al.*[14] made numerical analysis and experiments related to liquid gallium but in a finite domain. Other experiments were done by Wang and Huang[15] with salt water. Hughes and Griffiths[16] reviewed this problem including, among others, applications to oceanography.

The effect of an inclined temperature gradient was first investigated by Weber[17] assuming that the horizontal walls are stress-free and that the horizontal temperature gradient is small. Later, Sweet *et al.*[18] investigated the instability for free shear walls extending the results to larger values of the horizontal temperature gradient. They assume mean values of the basic velocity and temperature profiles, instead of the original z-dependent ones. It is found the possibility of oscillatory convection increasing the ratio of the applied temperature gradients. This problem is extended, with the same assumption but for small horizontal temperature gradient, to the case of rigid horizontal walls by Bhattacharyya and Nadoor.[19] Later, Weber[20] improved his calculations for stress-free walls using a Galerkin method. He also made calculations for rigid horizontal walls. He found that the Prandtl number is important to determine which mode is the first to appear in the instability, the longitudinal or the transversal one with respect to the basic flow. Besides, he shows that an increase of the horizontal temperature gradient promotes the appearance of oscillatory flow. Nield[21] was the first to try to give a more complete view of this phenomena for four different values of the Prandtl number. His goal was to investigate all the possible modes of instability by means of a Galerkin method. Due to numerical problems, his results were limited to a horizontal Rayleigh number of 6000. Later, Kaloni and Qiao[22] made calculations by means of the energy method. They showed that the curves of criticality of Nield[21] should drop to zero critical vertical Rayleigh number R_{VC} with the increase of R_H. Therefore, for some Prandtl numbers, the linear results of Nield[21] have to be corrected and extended to larger magnitudes of R_H.

In this paper, we present complete calculations of the linear problem of natural convection under an inclined temperature gradient. To reach this goal, the numerical method used by Nield is improved to get a better convergence and the magnitude[21] of R_H is extended up to a value where the curve of R_{VC} drops to zero and the flow is unstable only by means of a horizontal temperature gradient. Here, the magnitude of the Prandtl number will be restricted between the range of 0.026 and 1. The selection of this range is because there the qualitative properties of the curves of criticality have an important change that allows, in a certain range of R_H, for the appearance of the new oblique oscillatory mode of instability as the first unstable one, a result not presented before in the open literature. Moreover, it is shown that this qualitative change also leads to the appearance of an odd longitudinal stationary mode and a harmonic of the even longitudinal stationary mode as the first unstable in other different ranges of R_H. The paper is organized as follows. In Sec. II, a description of the physical system is given along with the equations of motion and energy with their linearized expressions for use in the numerical analysis. In Sec. III, a description of the numerical method is presented with a discussion on how this improves the one used by Nield.[21] Section IV gives the results in the form of plots of the critical vertical Rayleigh number R_{VC}, wavenumber α_C, frequency of oscillation σ_C, and angle of propagation of the perturbation ϕ_C against R_H. The plots of the streamlines are included to understand the physical behavior of the flow. Section V presents the discussion, and Sec. VI is the conclusions.

II. EQUATIONS OF MOTION

The system under investigation is a flat fluid layer subjected to an inclined temperature gradient. It is supposed that the lateral differentially heated vertical walls are very far away and that the region of interest is a large central part where the basic flow can be considered as parallel. The parallel flat walls that contain the fluid are very large in comparison to the thickness of the layer and are supposed to be perpendicular to gravity. The walls are very good conductors, and the lower wall is hotter than the upper one. This produces a vertical temperature gradient which combined with the horizontal one, results in an inclined temperature gradient. The fluid moves upwards in the hot lateral wall and goes downwards in the cold one. This generates a basic flow U(z) in the x-direction which depends on the vertical variable z. Perpendicular to the basic flow and to the z-direction is the y-direction. The equations are

$$Pr^{-1}\frac{D\bar{u}'}{Dt} = -\nabla p' + T'\mathbf{k} + \nabla^2\bar{u}', \tag{1}$$

$$\frac{DT'}{Dt} = \nabla^2 T', \tag{2}$$

$$\nabla\cdot\bar{u}' = 0, \tag{3}$$

where D/Dt is the Lagrange operator and use has been made of the Boussinesq approximation. Here, $\bar{u}' = (u', v', w')$ is the velocity vector, $\mathbf{k}$ is a vertical unit vector, p' is the pressure, and T' is the temperature. The variables have been made non dimensional using for distances the thickness of the layer d, for time d^2/κ (where κ is the thermal diffusivity), for velocity κ/d, for pressure $\rho_0\kappa\nu/d^2$ (where ρ_0 is a reference density) and for temperature $\Delta T/R_V$, where ΔT is the vertical temperature difference and the vertical Rayleigh number is defined as $R_V = g\alpha_T d^3\Delta T/\nu\kappa$. The horizontal Rayleigh number is defined as $R_H = R_V d\beta_H/\Delta T = g\alpha_T d^4\beta_H/\nu\kappa$, where β_H is the magnitude of the horizontal temperature gradient. The walls are rigid and good conductors, then the velocity and temperature satisfy the boundary conditions at the walls located at $z = \pm 1/2$

$$\bar{u}' = 0, \tag{4}$$

$$T' = \mp R_V/2 - R_H x. \tag{5}$$

In the inner region, very far from the lateral walls, the flow is assumed parallel, and the variables of the steady state solution only depend on z. Thus, the basic flow and temperature profiles satisfy the equations

$$D^3U(z) = -R_H, \tag{6}$$

$$D^3V(z) = 0, \tag{7}$$

$$D^2T(x,z) = -R_H U(z), \tag{8}$$

where $D = d/dz$ and $T(x, z) = F(z) - R_H x$. Therefore, the goal is to calculate F(z) by means of Eq. (8). Note that at $z = \pm 1/2$, $F(z) = \mp R_V/2$. The flow is closed and the velocity components U(z) and V(z) must satisfy a condition of zero mass flux, that is, the integral of U(z) and V(z) in the range of the thickness of the fluid layer must be zero. The solutions are

$$U(z) = R_H(z/24 - z^3/6), \tag{9}$$

$$V(z) = 0, \tag{10}$$

$$T(x,z) = R_H^2(7z/5760 - z^3/144 + z^5/120) - R_V z - R_H x. \tag{11}$$

The basic flow Eq. (9) modifies the temperature profile as in Eq. (11), producing two unstable regions near the upper and lower walls and a stable region in the middle section (see Fig. 1 of Lappa[23]). These unstable regions are made more unstable by an adverse vertical temperature gradient. This shows that for a large enough horizontal temperature gradient alone, it is possible to destabilize the flow. However, due to the stabilizing region of the temperature profile, it is not possible to destabilize the system for small R_H and the result is that R_H first stabilizes, for some magnitudes of the Prandtl number, in the presence of R_V and later destabilizes also due to the contributions of the shear flow instability. In another region, for Pr smaller than a critical magnitude calculated in this paper, R_H destabilizes even for small magnitudes, as will be seen presently. When $R_V > 0$, the two unstable regions in the temperature profile also bring about the possibility of having an odd mode as the first to appear in the instability, as will be shown below. The characteristic of this odd mode is that it produces two convection cells, one over the other. The stability of the flow is investigated using normal modes of the form $G(z)exp[i(kx + ly - \sigma t)]$, where $G(z)$ represents the amplitude of any of the perturbations of the variables and k and l are the x and y-components of the perturbation wavenumber. The real part of σ is the frequency of oscillation of the perturbation and its imaginary part is the growth rate. In this way, the system of equations of the perturbations is

$$[Pr(D^2 - \alpha^2) - i(kU - \sigma)](D^2 - \alpha^2)w + ikwD^2U - Pr\alpha^2\theta = 0, \tag{12}$$

$$[(D^2 - \alpha^2) - i(kU - \sigma)]\theta + R_H u - wDT = 0, \tag{13}$$

$$[Pr(D^2 - \alpha^2) - i(kU - \sigma)](-\alpha^2 u + ikDw) + l^2 wDU = 0, \tag{14}$$

where u and w are the amplitudes of the x and z-components of the velocity, respectively, and θ is the amplitude of the temperature. The square of the magnitude of the wavenumber vector is defined as $\alpha^2 = k^2 + l^2$. Therefore, it is possible to write $k = \alpha\cos\phi$ and $l = \alpha\sin\phi$, where ϕ is the angle of propagation of the perturbation with respect to the x-direction (the same of the basic flow). The boundary conditions are $w = Dw = u = \theta = 0$ at $z = \pm 1/2$.

The Eqs. (14) and (12) are obtained applying once and twice, respectively, the rotational operator to the perturbed equation of motion. Therefore, Eq. (14) corresponds to the vorticity equation. This system of equations will be analyzed numerically as explained in Sec III.

III. NUMERICAL ANALYSIS

The boundary value problem formed by the system of Eqs. (12)–(14) and the boundary conditions will be solved

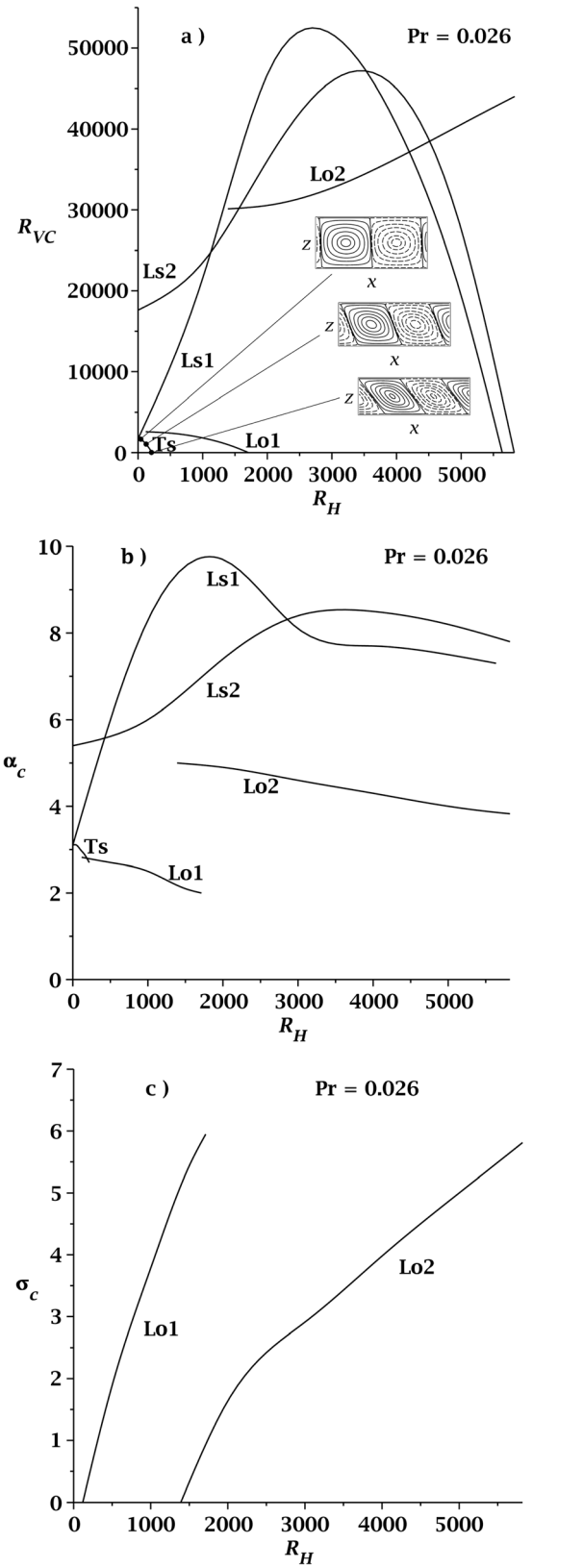

FIG. 1. Graphs of R_{VC} vs R_H for fixed $Pr = 0.026$. In (a), the areas below the curves are stable with respect to the corresponding critical instability. Here, the first unstable mode is T_S, the transversal stationary mode, and only below this curve the flow remains stable. The other modes L_{O1}, L_{O2}, L_{S1}, and L_{S2} are the longitudinal oscillatory even and odd modes and the longitudinal stationary even and odd modes, respectively. In (b) and (c), the critical wavenumber and frequency, respectively, are presented. Streamlines data are in the order (R_H, R_{VC}, α_C): T_S (10, 1703.03, 3.1), T_S (100, 1266.54, 3), and T_S (218.24, 0, 2.7).

by means of a Galerkin numerical method.[24,25] The accuracy of the solutions depend on the selected trial functions, which should satisfy the boundary conditions. Here, the selected functions will be characterized by having, at the same time, an even and an odd mode. This was done following the calculations of Hart[5] for horizontal temperature gradient alone, who found that it is possible to capture accurately different modes of instability when including even and odd trial functions. Notice that this was not done by Nield[21] who stops his analysis at a relatively small R_H due to problems of convergence in the calculations. Nield[21] pointed out that for some Prandtl number and for a range of R_H an oblique mode appears but that it was not the first one to appear in the instability. However, due to the Galerkin method used here, it has been possible to show, among other things, that an oscillatory oblique mode can be the first unstable one in a range of R_H and in a range of Pr. Note that numerically, it is only possible to separate the even and odd modes in the case of longitudinal perturbations and to obtain, from a solvability condition, a determinant in the form of a product of two terms, each one for each mode. Therefore, the calculations for all the other angles of propagation of the perturbation are more complicated.

The perturbation functions appearing in Eqs. (12)–(14) are expanded in the following form:

$$w = w_e + w_o = \sum_{n=1}^{N} [a_{2(n-1)} z^{2(n-1)} (z^2 - 1/4)^2 + b_{2n-1} z^{2n-1} (z^2 - 1/4)^2], \tag{15}$$

$$\theta = \theta_e + \theta_o = \sum_{n=1}^{N} [c_{2n-1} \cos(2n-1)\pi z + d_{2n} \sin 2n\pi z], \tag{16}$$

$$u = u_e + u_o = \sum_{n=1}^{N} [f_{2n-1} \cos(2n-1)\pi z + g_{2n} \sin 2n\pi z], \tag{17}$$

where the subindexes e and o mean even and odd functions, respectively. These expansions are used in their full expression when the perturbations are transversal and oblique. However, if the perturbations are longitudinal, it is possible to use only the even part for even perturbations and the odd part for odd perturbations. Note that the following notation will be used below: $W_n = z^n(z^2 - 1/4)^2$, $T_{2n-1} = \cos(2n-1)\pi z$, $T_{2n} = \sin 2n\pi z$, $U_{2n-1} = \cos(2n-1)\pi z$, and $U_{2n} = \sin 2n\pi z$.

Equations (15)–(17) are substituted into the homogeneous system of differential Eqs. (12)–(14). Then, the residuals are made orthogonal to the basic trial functions.[24,25] All this leads to a system of linear algebraic equations whose solution is only different from the trivial one if the determinant of the matrix of the system M is zero, that is, $det(M) = 0$. This matrix is of order $3(2N) \times 3(2N)$ and its elements are

$$M_{3i-2,3j-2} = \langle L_1 W_j, W_i \rangle, \quad M_{3i-2,3j-1} = -\alpha^2 \langle T_j, W_i \rangle,$$
$$M_{3i-2,3j} = 0, \quad M_{3i-1,3j-2} = \langle DTW_j, T_i \rangle,$$
$$M_{3i-1,3j-1} = \langle L_2 T_j, T_i \rangle, \quad M_{3i-1,3j} = -R_H \langle U_j, T_i \rangle,$$
$$M_{3i,3j-2} = \langle L_4 W_j, U_i \rangle, \quad M_{3i,3j-1} = 0, \quad M_{3i,3j} = \langle L_3 U_j, U_i \rangle.$$

From the equation $det(M) = 0$, it is possible to obtain the proper values of R_V and σ in terms of α, ϕ, R_H, and Pr. To find them, use has been made of a Newton-Raphson method[26] implemented in the Maple algebra package.

As shown below, the instability of the oblique mode of instability will be investigated. The calculation of this mode requires to check around the 360° of the direction of propagation of the perturbation. A lot of work can be saved by reviewing the symmetry properties of Eqs. (12)–(14). First use is made of the definitions $k = \alpha \cos\phi$, $l = \alpha \sin\phi$, and $\alpha^2 = k^2 + l^2$. Now, Eqs. (12)–(14) will be subjected to two rotations. The first one is $\phi \to -\phi$ (with respect to the basic flow x-direction) which only changes $l \to -l$, but l only appears squared in all the equations. This means that the equations remain the same and so will be the stability results. The second one is a rotation $\phi \to \phi + \pi$ which produces the changes $l \to -l$ and $k \to -k$. Proposing in this case, the changes $U_S \to -U_S$, $u \to -u$, and $R_H \to -R_H$, it is possible to recover the original system of equations. The reason is that a 180° rotation is equivalent to changing the direction of the x-axis. Therefore, a change of the directions of the basic flow, the horizontal temperature gradient, and the velocity perturbation in the x-direction gives the same Eqs. (12)–(14). In conclusion, for the oblique instability, it is only needed to investigate the first quadrant of the wavenumber plane. Even with this simplification, the stability calculations are very time consuming.

Some useful analytical results for the marginal R_V are given by the following equations obtained from the smallest order Galerkin approximation. They correspond to the longitudinal instability case ($k = 0$, $l = \alpha$) in which the even and odd modes separate easily and simultaneously obtain the two algorithms corresponding to the solutions of those two instability modes. They are valid for relatively small magnitudes of R_H. They are first, for the stationary longitudinal even mode

$$R_V = \frac{1}{20160} \frac{(\alpha^4 + 24\alpha^2 + 504)(\alpha^2 + \pi^2)\pi^{10}}{C_1^2 \alpha^2} + \frac{1}{720\pi^2 C_1} \left(\frac{A_1}{\pi^2} + \frac{60 B_1}{(\pi^2 + \alpha^2) Pr} \right) R_H^2, \tag{18}$$

and second, for the oscillatory longitudinal even mode

$$\sigma^2 = \frac{1680 Pr \alpha^2 B_1 C_1 R_H^2}{\pi^{12}[(\alpha^4 + 24\alpha^2 + 504)Pr + (\alpha^2 + \pi^2)(\alpha^2 + 12)]} - (\alpha^2 + \pi^2)^2 Pr^2, \tag{19}$$

$$R_V = \frac{1}{20160} \frac{[\alpha^4 + 24\alpha^2 + 504 + (\alpha^2 + \pi^2)(\alpha^2 + 12)](\alpha^2 + \pi^2)(1 + Pr)\pi^{10}}{C_1^2 \alpha^2} + \frac{1}{720\pi^2 C_1} \left\{ \frac{A_1}{\pi^2} - \frac{60 B_1 (\alpha^2 + 12)}{[(\alpha^4 + 24\alpha^2 + 504)Pr + (\alpha^2 + \pi^2)(\alpha^2 + 12)]} \right\} R_H^2 \tag{20}$$

and use was made of $A_1 = \pi^6 + 348\pi^4 - 64800\pi^2 + 604800$, $B_1 = \pi^4 - 228\pi^2 + 2160$, and $C_1 = 12 - \pi^2$. Here, σ is the frequency of oscillation. The corresponding odd modes are omitted because they are very stable for small R_H and are not relevant in what follows.

It is important to point out that the numerical method used here made it possible to have very good convergence increasing the order of approximation as needed. The results were compared with the limiting case of horizontal temperature gradient alone which was investigated numerically by Kuo *et al.*,[7,8] Laure,[10] Laure and Roux,[11] and Kaddeche *et al.*[27] (when the magnetic field is zero). The agreement was very good.

IV. NUMERICAL RESULTS

The stability results will be presented in order of increasing the Prandtl number. The first results are for $\mathrm{Pr} = 0.026$, which correspond to liquid metals like Mercury at 20 °C (Ref. 28) and Gallium at 30 °C.[4] Figure 1(a) shows the critical values of R_V, that is R_{VC}, against R_H for $\mathrm{Pr} = 0.026$. Different modes of instability are presented for the sake of completeness. Modes that are not important here because they are more stable than the critical one, will be important for larger values of Pr. In Fig. 1, the instability is dominated by a transversal stationary mode T_S which attains the value of $R_{VC} = 1708$ when $R_H = 0$. For this Pr, the curve drops to $R_{VC} = 0$ with a relatively small $R_{HC} = 218.25$ and a wavenumber $\alpha_C = 2.7$. The longitudinal oscillatory even mode L_{O1} drops at $R_{HC} = 1712.30$, $\alpha_C = 2.0$, and $\sigma_C = 5.94$. It was possible to capture a longitudinal oscillatory odd mode L_{O2}, but R_{VC} increases with R_H and it seems that it never destabilizes. The curves for the stationary longitudinal even L_{S1} and odd L_{S2} modes are of particular interest because they stabilize in an important way in some region of R_H, but later destabilize dramatically for large values of R_H. This behavior will have important consequences for larger Pr. The curve of L_{S1} also tends to $R_{VC} = 1708$ when R_H goes to zero. Notice that the modes L_{O1} and L_{O2} start for a magnitude of R_H different from zero, as it should be because it is well known that when $R_H = 0$, the instability begins as stationary.[1] Therefore, there is a critical value of R_H after which the curves of these modes start. The streamlines of the flow at criticality of two representative sets of (R_H, R_{VC}, α_C) are also shown in the figure. They are the streamlines of a stationary transversal mode and correspond to the values (10,1703.03,3.1), (100, 1266.54, 3) and (218.24, 0, 2.7), respectively. It is clear that the convection cells show no symmetry with respect to z = 0 (located at the middle of the z-axis), as explained above.

Figure 2 presents results for $Pr = 0.2$ which corresponds approximately to a mixture[29] of molten Lead (44.5%) and Bismuth (55.5%) at 644 °C. Due to the changes of the curve T_S with respect to the Prandtl number, some important results appear in this figure. First, the T_S curve starts to grow and the system stabilizes taking magnitudes of R_{VC} larger than 1708 in almost all its range of R_H and then drops to $R_{VC} = 0$ at $R_H = 5089.81$. Second, a codimension two point appears at approximately $R_{VC} = 2652$ and $R_H = 1010$, where stationary (T_S) and oscillatory (L_{O1}) convective motions compete

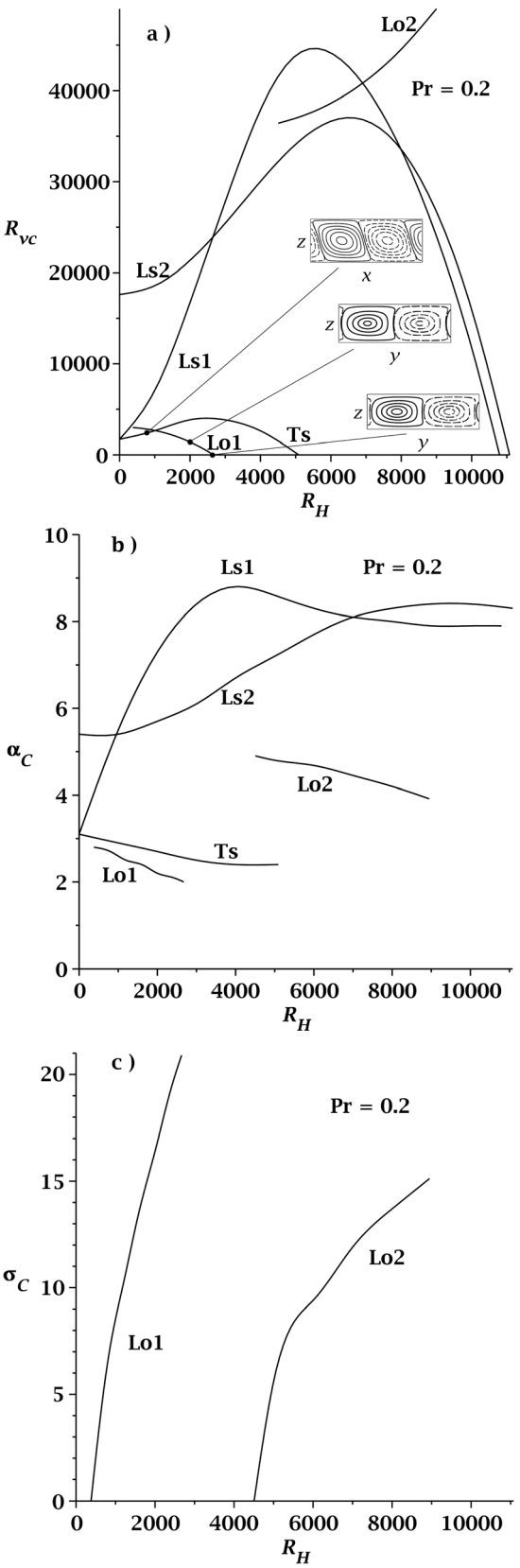

FIG. 2. Graphs of R_{VC} vs R_H for fixed $Pr = 0.2$. In (a), the areas below the curves are stable with respect to the corresponding critical instability. Here, the first unstable mode is T_S and then the mode L_{O1}. A codimension two point appears at around $R_H = 1010$ and $R_V = 2652$, larger than 1708. The other modes L_{O1}, L_{O2}, L_{S1}, and L_{S2} appear again as more stable. In (b) and (c), the critical wavenumber and frequency, respectively, are presented. Streamlines data are in the order (R_H, R_{VC}, α_C, σ_C): T_S (800, 2351.21, 2.9, 0), L_{O1} (2000, 1404.83, 2.2, 16.46), and L_{O1} (2671.40, 0, 2, 20.90).

for instability. These results are new and have not been reported before in the open literature. Then, only below these two curves, the flow remains stable. The curve of L_{O1} falls to $R_{VC}=0$ at $R_H=2671.40$. It is clear that modes L_{S1} and L_{S2} have broaden their stable area. The wavenumber of L_{O1} remains smaller than that of T_S. Here, the streamlines for three representative flows are given for three sets of four values (R_H, R_{VC}, α_C, σ_C). The flow for (800, 2351.21, 2.9, 0) corresponds to T_S and, therefore, has no symmetry. The oscillatory mode is longitudinal and its symmetry for the values set (2000, 1404.83, 2.2, 16.46) is apparent. The curve L_{O1} for (2671.40, 0, 2, 20.90) is symmetric and has a smaller wavenumber. As seen in Fig. 2(a), the transversal convection cells are periodic in the x-direction, and the longitudinal cells are periodic in the y-direction. Notice that the wavenumbers of the convection cells of each case are different, but this was not taken into account when deciding the size of each figure of the streamlines. The main reason is that the relative scaling of the wavenumber made it impossible to see the separation of the streamlines in some cases of convection cells. Here, and in all the figures, it is interesting to note that, for small magnitudes of R_H, the curves L_{O1} disappear before $R_H=0$. The reason is that for small magnitudes of R_H it is not possible to find roots of the frequency of oscillation in agreement with the results of vertical temperature gradient alone, where it has been shown that stationary convection is the first to appear.[1] It is also clear that the curves of L_{O1} do not reach those of L_{S1} in Figs. 1(a) and 2(a).

The codimension two point begins to appear when the curves of T_S and L_{O1} touch each other for the first time at $R_{VC}=0$ and $R_{HC}=2249.05$ when $\mathrm{Pr}=0.1364$, as shown in Fig. 3 and confirmed by Kuo *et al.*[7,8] (case $R_V=0$). This critical magnitude of Pr is just that after which the pure T_S mode

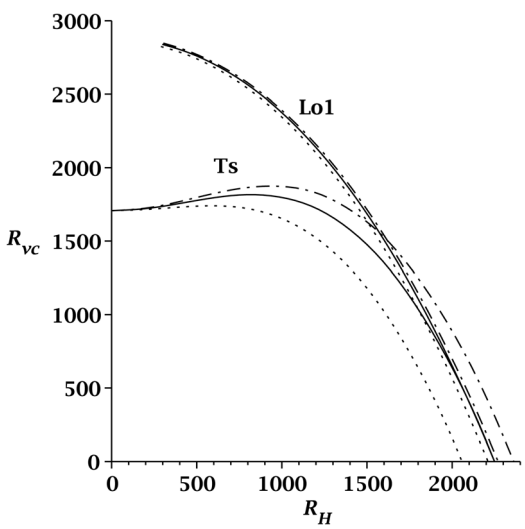

FIG. 3. Graphs of R_{VC} vs R_H for T_S and L_{O1} alone. The graphics are for three values: $Pr=0.13$ (dotted line), $Pr=0.1364$ (solid line), and $Pr=0.14$ (dashed dotted line). Notice that $Pr=0.1364$ is the critical Prandtl number at which the first codimension two point appears when $R_V=0$ and $R_{HC}=2249$. For larger values of Pr, the codimension two points appear for $R_V>0$. Thus, mode L_{O1} can be the first unstable one, only for $\mathrm{Pr}>0.1364$ and above a critical R_H, to the right of the codimension two point. For example, for $\mathrm{Pr}=0.14$ (dashed dotted line) that point is located at $R_H=1620$ and $R_{VC}=1503$.

changes in such a way that it allows for another instability mode to appear as the first unstable one for larger Pr, that is, the mode L_{O1}. It is very interesting to point out that, in the presence of R_V, it is possible to have this codimension two point in a range of Pr, starting from $\mathrm{Pr}=0.1364$, in contrast with the case of R_H alone. Moreover, notice in Fig. 3 that very near to $\mathrm{Pr}=0.13$, the curve of T_S starts to create a stabilizing bump which shows the above mentioned stabilizing effect of R_H in an important range. This stabilizing effect on T_S is the cause of the appearance of the codimension two point, because it delays the drop of the curve into a larger critical R_{HC}, which increases faster than that of the curve L_{O1} with respect to Pr. Notice that the magnitude of R_H of the codimension two point decreases with Pr, as seen in Figs. 3 and 2. For example, for $\mathrm{Pr}=0.14$, $R_H=1620$, and $R_{VC}=1503$ and for $\mathrm{Pr}=0.2$, $R_H=1010$, and $R_V=2652$. The reason is the constant increase with Pr of the bump of the curve of T_S.

The results shown in Fig. 4 correspond to $\mathrm{Pr}=0.45$ (Fig. 4(a)) and 0.4886 (Fig. 4(b)). In Fig. 4(a), it is shown the important result of the presence of the new oblique oscillatory mode Ob_O. It seems that the curve of Ob_O starts to appear somewhere inside the range $0.2<\mathrm{Pr}<0.45$. Therefore, the first unstable modes for $\mathrm{Pr}=0.45$ are a stationary transversal mode, an even oscillatory longitudinal mode and an oblique oscillatory mode. The first codimension two point in this figure, between T_S and L_{O1}, occurs at $R_H=1105$ with the following data ordered as R_V, α, and σ (3589, 2.9, 0) and (3589, 2.7, 10.43), respectively. The mode Ob_O starts to be the first unstable one at $\phi=86^\circ$ when $R_H=8300$ and (1582.34, 1.4, 60.38) and it crosses the $R_V=0$ axis at $R_H=9935$ and (0, 1.6, 83.67) when $\phi=72^\circ$. The results of Fig. 4(b) for $\mathrm{Pr}=0.4886$ are interesting because a new codimension two point appears when the curves of Ob_O and L_{S1} touch each other when $R_H=12329.5$ for (0, 1.7, 115.32) at an angle of 65° and for (0, 8.2, 0), respectively. Here, again Ob_O starts to be the first unstable one at $\phi=86^\circ$ but when $R_H=7800$ and (4378.81, 1.5, 60.99). Notice that the slope of L_{O1} already changed in this figure. This is important for other phenomena which appear for larger Pr because the slope of Ob_O will also change following that of L_{O1}.

The way an oblique mode is calculated is by searching around any stationary or oscillatory curve of criticality if there are more unstable modes at different angles of the wavenumber of the perturbation. Calculations show that the Ob_O curve of criticality is first found separating from the curve L_{O1} near but below $Pr=0.45$ (see Fig. 4). This curve also appears for $Pr=0.5$ (Fig. 5(a)) and for $Pr=1$ (Fig. 6(a)). For example, in the case of $Pr=1$, the separation of the curve of Ob_O from that of L_{O1} is better understood by means of the behavior of the marginal curves. The curve starts to separate from a value of R_H between 6700 and 6750 and the marginal curve begins to show two minima one of which is the absolute one corresponding to L_{O1}. A further increase of R_H decreases the difference between the two minima until $R_H=6785$, where both minima reach the same magnitude of R_V. At this point, two convection cells of two different wavenumbers (with small difference between each other) and two different frequencies compete to be the first

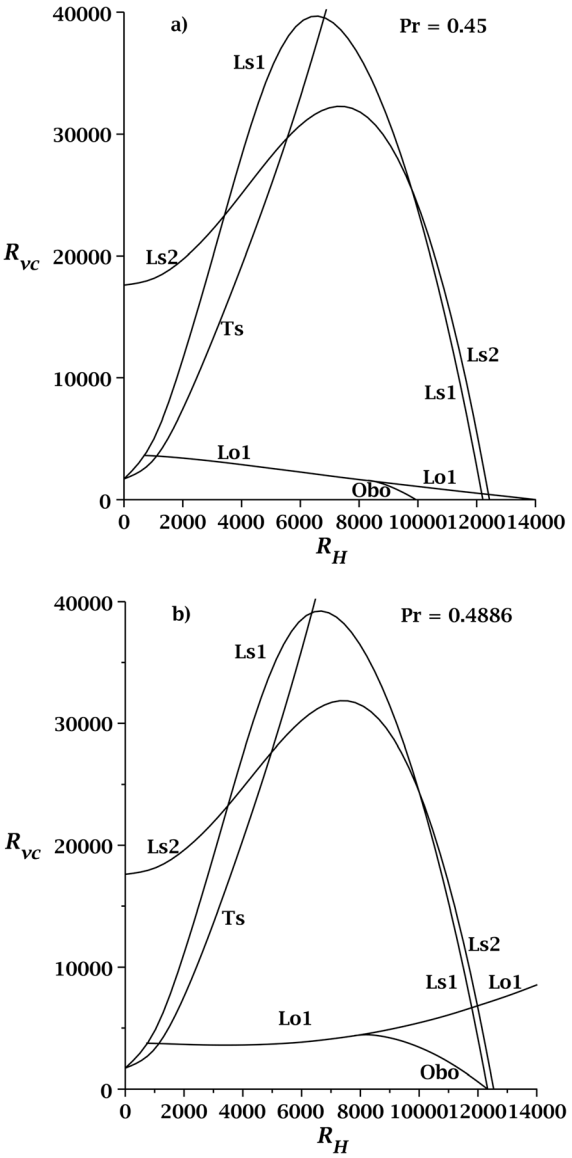

FIG. 4. Graphs of R_{VC} vs R_H for (a) $Pr = 0.45$ and (b) $Pr = 0.4886$. (a) Results previous to the codimension two point. It is of interest to note that the oblique mode is already present. (b) For Prandtl number 0.4886, a new codimension two point between Ob_O and L_{S1} appears for $R_{VC} = 0$ and $R_H = 12330$. Besides, notice that the curve of L_{O1} already changed its slope, fact that will be important for larger Pr because the curve of Ob_O will also follow this behaviour.

unstable one. Finally, another increase of R_H makes the mode Ob_O to be the first unstable one.

Figure 5 shows results for $\mathrm{Pr} = 0.5$, which may correspond to a mixture of air and H_2 from 20% to 50%.[28] The further increase of the Prandtl number leads to a rise of the curve of L_{O1} which produces a change in that of Ob_O. This behaviour makes the new codimension two point between Ob_O and L_{S1} to have a R_V different from zero. At the same time, this produces a decrease of the corresponding R_H of the crossing point. In particular for $\mathrm{Pr} = 0.5$, that point is located at $R_H = 12244$ for (1464.59, 1.7, 115.13) at $\phi = 65°$ (Ob_O mode) and for (1464.59, 8.2, 0) (L_{S1} mode), respectively. With this changes, the even stationary longitudinal mode L_{S1} becomes the first unstable one in a range of R_H, as seen in Fig. 5(a). This curve hits the $R_V = 0$ axis at $R_H = 12359$ for (0, 8.2, 0). The Ob_O mode starts to appear as the first unstable one when $R_H = 7730$ for (5066.46, 1.5, 60.57) at $\phi = 89°$. The first codimension two point between T_S and L_{O1} occurs at $R_H = 1147$ with (3764.7, 2.9, 0) and (3764.7, 2.7, 10.83), respectively. The results for the critical wavenumber are shown in Fig. 6(b). It is clear that the wavenumber of L_{O1} remains below that of T_S and Ob_O. The critical frequency of oscillation of L_{O1} shown in Fig. 5(c) increases with respect to the case of $\mathrm{Pr} = 0.2$ and that of Ob_O is even more larger. As can be seen in Fig. 5(d), the critical angle of propagation of the perturbation shows discontinuous jumps due to the competition between pairs of modes. The first one is that between T_S and L_{O1}, then between L_{O1} and Ob_O (small), and finally between Ob_O and L_{S1}.

Figure 6 shows the results for $\mathrm{Pr} = 1$ corresponding approximately to gases and vapor at 200 °C (Ref. 28) and one atmosphere. With this figure, it is possible to compare with the results of Nield.[21] It is important to note the increase of the range of R_H used in the calculations. The results of Fig. 6(a) show that increasing R_H starting from zero, the first unstable mode is T_S, then at $R_H = 1563$, the mode is L_{O1}, next from $R_H = 6785$ appears the new oscillatory oblique mode Ob_O, which is followed from $R_H = 8957$ by the odd longitudinal stationary mode L_{S2}, and finally from $R_H = 11020$, the first unstable one is the even longitudinal stationary mode L_{S1}. The different curves intersect to each other at important points whose data will be ordered as R_V, α, and σ. Two codimension two points appear for this Prandtl number. The first one was already found by Nield[21] and from our numerical results it occurs at $R_H = 1563$ and (5659, 2.7, 0) for T_S and (5659, 2.8, 12.87) for L_{O1}. The other appears at $R_H = 8957$ and (27714, 2.4, 124.52) for Ob_O when $\phi = 60°$ and (27714, 7.4, 0) for L_{S2}. Notice that this is a new codimension two point due to the surprising presence of the odd mode L_{S2} as the first unstable one in a range of R_H. Other points are of importance. The intersection between L_{S1} and L_{S2} is located at $R_H = 11020$ and (19221, 8.1, 0) for L_{S1} and (19221, 8.1, 0) for L_{S2} (that is correct, they have the same wavenumber in this case). The mode L_{S1} finishes when touching the horizontal axis at $R_H = 12998$ and (0, 8.3, 0). These are curves of criticality and only below them the flow remains stable. As pointed out above, the mode Ob_O starts to appear between $R_H = 6700$ and 6750.

As can be seen, for $\mathrm{Pr} = 1$, the magnitudes of R_{VC} for all the critical curves are very large in comparison with 1708, which shows the great stabilizing effect of R_H. Therefore, this strong effect of R_H is the reason why the very highly stable odd mode L_{s2} has been reached by mode Ob_O to become the first unstable one in a range of R_H. Also shown, for reference, is the stability curve of the transversal oscillatory mode T_O. In Fig. 6(b), it is interesting to observe that the critical wavenumbers of mode L_{O1} are now larger than those of T_S, but smaller than those of mode Ob_O. The critical frequencies of Ob_O are also larger than those of L_{O1}, as seen in Fig. 6(c).

Figure 6(d) presents the critical angle of propagation of the perturbation ϕ_C. Note in the figure that this angle only starts as the first unstable one at around $\phi_C = 75°$ for $R_H = 6785$ and finishes at around $\phi_C = 60°$ for $R_H = 8957$, after which the mode L_{S2} is the first unstable one. The two

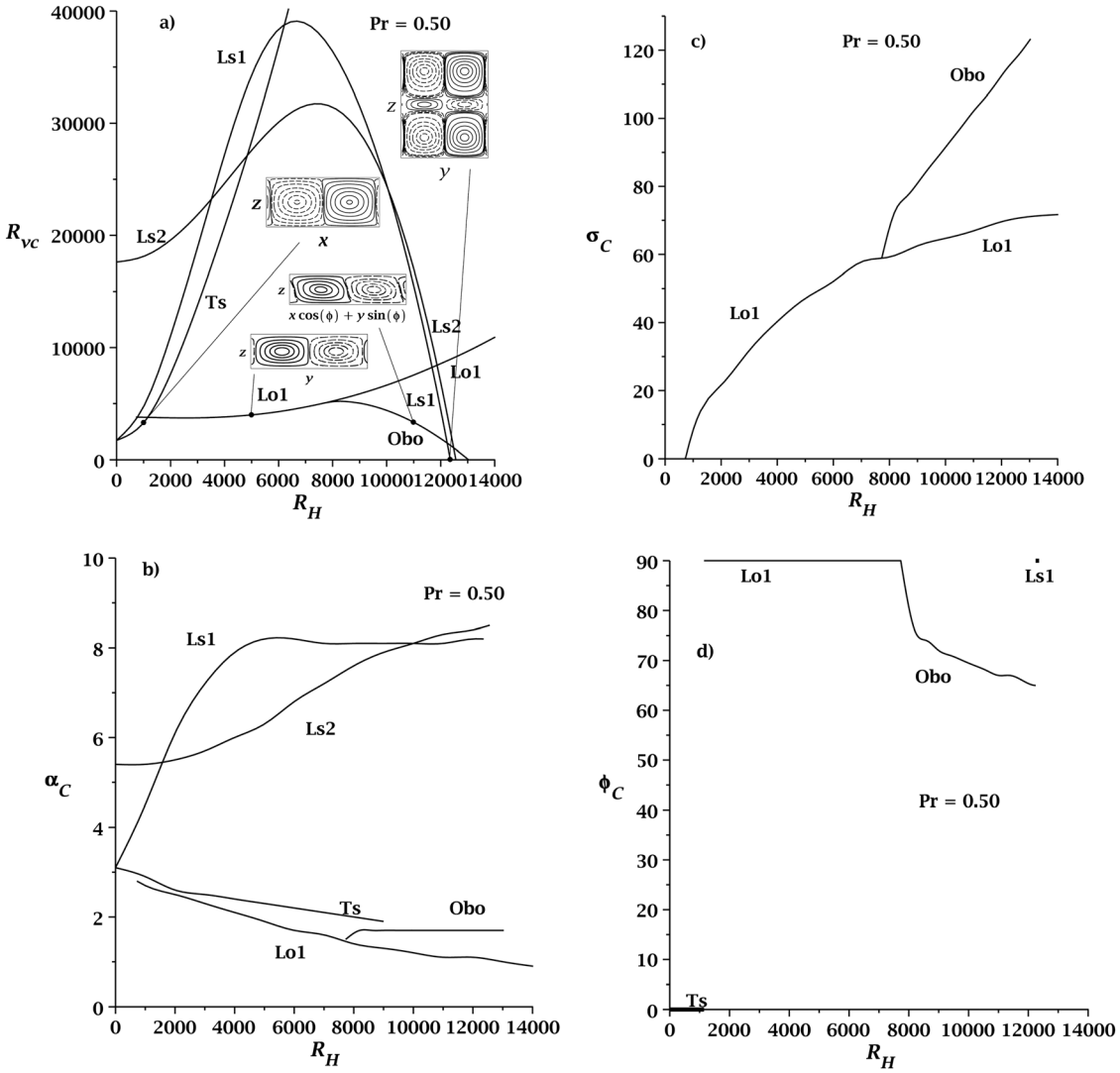

FIG. 5. Graphs of R_{VC} vs R_H for fixed $Pr = 0.5$. Here, increasing R_H from zero, the first unstable mode is T_S, then from $R_H = 1147$, the mode L_{O1}, next from $R_H = 7730$, a new oscillatory oblique mode Ob_O which is followed from $R_H = 12244$ by the even stationary mode L_{S1}. Note that, at the end, L_{S1} drops at $R_{HC} = 12358$. Two codimension two points appear from the competition between stationary and oscillatory modes and are located at around $R_H = 1147$ and $R_H = 12244$, respectively. In (b), (c), and (d), the critical wavenumber, frequency of oscillation, and angle of propagation of the perturbation, respectively, are presented. Streamlines data are in the order (R_H, R_{VC}, α_C, σ_C): T_S (1000, 3279.64, 2.9, 0), L_{O1} (5000, 3987.34, 1.9, 47.16), Ob_O (11000, 3327.59, 1.7, 102.12) at 67° and L_{S1} (12358.81, 0, 8.2, 0).

dashed lines indicate the angles of existence of the oblique mode but where it is no longer the first unstable one. It is of interest to point out that the oblique mode starts from a R_H larger than the largest magnitude investigated by Nield[21] in his Fig. 4. Thus, broadening the range of R_H has been of great importance in the present research because it also has been possible to show that the odd longitudinal stationary mode can be the first unstable one, followed by the even longitudinal stationary mode.

V. DISCUSSION

A variety of results have been presented in the above sections. Here, a discussion is given of the stability. An important characteristic of the flow under an inclined temperature gradient is the basic temperature profile given in Eq. (11). This equation is of 5th degree in z, in contrast to that of natural convection inside inclined parallel walls where the temperature profile is linear. Therefore, different results are expected even though the velocity profiles are similar.

The z-dependent part of the temperature profile Eq. (11) has five roots. It crosses through $z = 0$, which can be shown to be always an inflexion point. There are other four roots, two of them are outside the flow range of z, and the other two, calculated from $z^2 = (5R_H - 2\sqrt{R_H^2 + 4320R_V})/12R_H$, exist if $5R_H - 2\sqrt{R_H^2 + 4320R_V} \geq 0$, that is, when $R_H^2 \geq 5760R_V/7$. Note that, when the equality is satisfied, $z = 0$ becomes a root of multiplicity three and the other roots remain outside the range of z. The z-derivative of the temperature has two roots in the range of z, calculated from $z^2 = (15R_H - 2\sqrt{30R_H^2 + 21600R_V})/60R_H$, and exist if $15R_H - 2\sqrt{30R_H^2 + 21600R_V} \geq 0$, which corresponds to $R_H^2 \geq 5760R_V/7$, the same condition as that for the temperature. The second derivative of the temperature is $d^2T/dz^2 = R_H^2 z(z^2 - 1/4)/6$, which shows that $z = 0$ is the

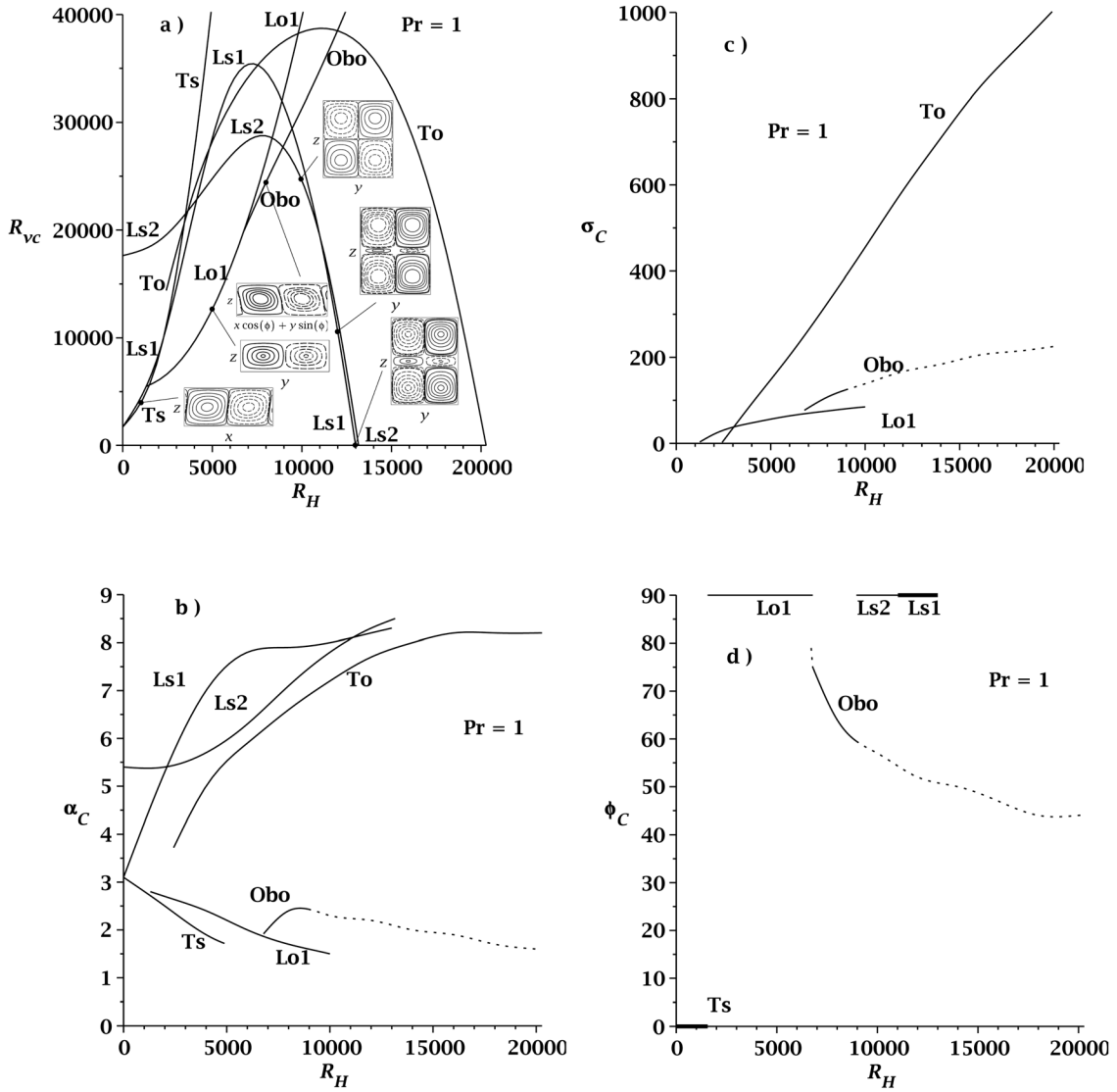

FIG. 6. Graphs of R_{VC} vs R_H and $Pr = 1$. The first unstable mode is T_S, then from $R_H = 1563$, the mode L_{O1}, next from $R_H = 6785$, a new oscillatory oblique mode Ob_O, followed from $R_H = 8957$ by the odd stationary mode L_{S2} and finally from $R_H = 11020$ is the even stationary mode L_{S1}. Note that L_{S1} drops at $R_{HC} = 12998$. Two codimension two points appear from the competition between stationary and oscillatory modes and are located at around $R_H = 1563$ and $R_H = 8957$, respectively. In (b), (c), and (d), critical wavenumber, frequency of oscillation, and angle of propagation of the perturbation, respectively, are presented. Streamlines data are in the order (R_H, R_{VC}, α_C, σ_C): T_S (1000, 3319.29, 2.9, 0), L_{O1} (5000, 12646.39, 2.2, 56.68), Ob_O (8000, 24448.55, 2.4, 107.54) at 64°, L_{S2} (10000, 24583.05, 7.8, 0), L_{S1} (12000, 10575.26, 8.2, 0), and L_{S1} (12998.04, 0, 8.3, 0).

inflexion point in the range of z. Notice that if the condition $R_H^2 \geq 5760 R_V/7$ is satisfied, a maximum appears in $0 < z < 1/2$ and a minimum exists in $0 > z > -1/2$. If these conditions are not satisfied, only an inflexion point is present and the temperature decreases monotonically with z. This is important, because only one convection cell is able to form inside the walls.

When the conditions are satisfied, the temperature profile shows two unstable regions inside the two walls due to the appearance of the maximum and minimum. The unstable regions are formed as follows. The first one is formed with the temperature difference between the point of the maximum and the upper wall and the second one with the temperature difference between the lower wall and the point of the minimum. This has an important consequence. That is, the formation of a very stable region in the middle section, between the point of the maximum (above) and the point of the minimum (below). This contributes to stabilize the flow when R_H increases, as seen in the curves of criticality of the results presented above when the Prandtl number is large enough (lets say, starting from $Pr = 0.2$). This stable region is responsible of the need to increase R_H to a magnitude far more larger than that required by the condition $R_H^2 \geq 5760 R_V/7$ in order to excite other modes of instability. Note that, in absolute value, the z-location of the maximum and minimum is reduced when R_H increases (see above, the location of the roots of the temperature derivative). Consequently, the stable region thickness decreases with R_H in such a way that, with the two unstable regions, it is possible to excite the odd mode (see the two cells streamlines of the odd longitudinal stationary mode L_{S2} in Fig. 6(a)) and to excite a harmonic mode of the even solution (see the three cells streamlines of the longitudinal stationary even mode L_{S1} in Fig. 5(a) ($R_V = 0$) and in Fig. 6(a) (for both $R_V = 0$ and $R_V > 0$)).

Among the properties of the eigenfunctions[30] that of symmetry is very important. The symmetry is reflected in the parity of the functions. An arbitrary function $f(z)$ can be decomposed into the sum of two functions of definite parity, even and odd with respect the origin.

The terms $(z^2-1/4)^2 z^{2(i-1)}$, with i an integer (see Eq. (15)), and the cosines of odd degree $\{\cos(\pi z), \cos(3\pi z), \ldots\}$ are even functions symmetric about the origin (Eqs. (16) and (17)). The terms $(z^2-1/4)^2 z^{2i-1}$, with i an integer, and the sines of even degree $\{\sin(2\pi z), \sin(4\pi z), \ldots\}$ are odd functions antisymmetric about the origin.

As can be seen, Eqs. (9) and (11) of the basic flow and temperature fields are odd functions of z. In Eqs. (12)–(14) of the perturbation appear the basic velocity (odd), its first derivative (even), its second derivative (odd), and the first derivative (even) of the basic temperature. With these symmetry characteristics, it is possible to prove that the equations for longitudinal disturbances ($k=0$, $l=\alpha$) are symmetric or antisymmetric if w, u, and θ are symmetric or antisymmetric, respectively. The reason is that, only in this case, the coefficients of the differential equations have even parity. Therefore, for the longitudinal disturbances, it is not necessary to combine even and odd solutions.[3] In order to calculate, the even longitudinal mode only the even functions and for the odd longitudinal mode only the odd functions of Eqs. (15)–(17) are required, respectively. Note that for all other orientations the even and odd modes remain coupled and the complete expressions in Eqs. (15)–(17) must be used.

The symmetries with respect to $z=0$ of these modes can be observed clearly by means of the convection cells streamlines of the longitudinal modes. For instance, when $Pr=1$ in Fig. 6(a), the mode Ls2 shows antisymmetry (odd parity). Besides, the modes Lo1 and Ls1 are symmetric (both have even parity). For the transverse and oblique modes, there is no symmetry, as can be seen from the complete Eqs. (12)–(14) and from the corresponding streamlines of the cells shown in Figs. 1(a), 2(a), 5(a), and 6(a).

As discussed before, the curves of criticality present codimension-two points at different magnitudes of R_H. In the figures, other curves above the first unstable ones present codimension-two points (see Figs. 1(a) and 2(a)); however, they are not important from the point of view of the linear theory. Only those occurring between critical curves are of interest and were discussed above. Note that all the curves above the critical in the figures are drawn as reference in order to understand their behavior before they become the first unstable when Pr increases.

VI. CONCLUSIONS

In this paper, new results of the problem of natural convection under an inclined temperature gradient have been presented. All the results calculated with the improved Galerkin method have been checked with those in the literature related with a horizontal temperature gradient. Besides, the results were also checked using a 5th order in the approximation of the Galerkin method. That is, ten terms (5 even and 5 odd) of the expansion of the variables were used. The broadening of the range of R_H in comparison with that used by Nield[21] lead to the interesting results presented here for the first time. The dominant mode for Prandtl numbers in the range $0.026 \leq \mathrm{Pr} \leq 0.1364$ is the transversal stationary. A codimension two point, due to the competition between stationary and oscillatory modes, appears at $\mathrm{Pr}=0.1364$ for $R_{VC}=0$, where the curves of T_S and L_{O1} touch each other for the first time. The presence of a vertical temperature gradient, represented by R_V, promotes the appearance of this codimension two point for all the Prandtl numbers in the range $0.1364 < \mathrm{Pr} \leq 1$. This codimension two point starts to appear due to the increase with Pr of the stabilizing bump in the curve of T_S which eventually allows the mode L_{O1} to be the first unstable one. The same behavior of this two curves follows until a critical value of Pr is reached after which their slopes change and it is found that they do not drop to $R_V=0$ in the range of R_H investigated. This critical value of Pr for T_S is different from that of L_{O1}. For T_S, it is nearly $\mathrm{Pr}=0.4$ (here corrections are given to the work of Kuo *et al.*[7,8]) and for L_{O1}, it is approximately $\mathrm{Pr}=0.46$. These two Prandtl numbers are very important because for magnitudes above them, the rapid growth of T_S and L_{O1} with R_H is determinant for the appearance of other modes as the first unstable ones in the instability. However, before the change of slope of L_{O1} occurs, there is a Prandtl number after which the new oblique oscillatory mode starts to appear. With a further increase of Pr, this mode is able to intersect the curve of L_{S1} producing another new codimension two point. This codimension two point still appears until a Prandtl number between 0.5 and 1 where another new codimension two point appears at the cross point between the oblique oscillatory mode and the odd mode L_{S2} which now appears as the first unstable one in a range of R_H. This mode L_{S2} is ignored in the case of vertical temperature gradient alone ($R_H=0$) due to its very high stability. However, due to the strong stabilizing effect of R_H on the different modes of the instability, this mode is now able to be the first one to destabilize in a range of R_H.

The streamlines of the convection cells for representative magnitudes of R_H and R_{VC} have been included in the figures. With them, it is possible to understand physically the qualitative and quantitative changes of the cells under the influence of the different parameters involved in the system of equations. The important effect of the basic temperature profile on the structure of the convection cell is clear when the maximum and minimum have a large enough temperature difference with respect to the walls at large R_H. With this, it was shown that it is possible to excite convection modes not seen before like the odd L_{S2} mode (two cells) and the harmonic of the even L_{S1} mode (three cells). These results are new in the presence of an inclined temperature gradient.

Detailed calculations for the Prandtl numbers larger than $\mathrm{Pr}=1$ are in progress and are not presented here. Our hope is to find new critical modes. However, it is also of interest to follow the oblique oscillatory mode and to find out the maximum Prandtl number where it can appear as the first unstable one. This requires far more careful calculations.

ACKNOWLEDGMENTS

The authors would like to thank Joaquín Morales, Cain González, Raúl Reyes, Ma. Teresa Vázquez, and Oralia

Jiménez for technical support. A. S. Ortiz-Pérez would like to thank the support of CONACyT through its scholarship program with number 208242/202097.

[1]S. Chandrasekhar, *Hydrodynamic and Hydromagnetic Stability* (Dover, New York, 1981).
[2]D. T. J. Hurle, E. Jakeman, and C. P. Johnson, "Convective temperature oscillations in molten gallium," J. Fluid Mech. **64**, 565 (1974).
[3]J. E. Hart, "Stability of thin non-rotating Hadley circulations," J. Atmos. Sci. **29**, 687 (1972).
[4]A. E. Gill, "A theory of thermal oscillations in liquid metals," J. Fluid Mech. **64**, 577 (1974).
[5]J. E. Hart, "A note of stability of low-Prandtl-number Hadley circulations," J. Fluid Mech. **132**, 271 (1983).
[6]I. C. Walton, "The effect of a shear flow on convection near a two-dimesional hot-patch," Q. J. Mech. Appl. Math. **38**, 561 (1985).
[7]H. P. Kuo, S. A. Korpela, A. Chait, and P. Marcus, "Stability of natural convection in a shallow cavity," in *Proceedings of the 8th International Heat Transfer Conference* **4**, 1539, edited by C. L. Tien (Hemisphere Pub. Corp., Washington, DC, 1986), Vol. 4, p. 1539, Report Nos. IRN13660664 and ISBN0891165592.
[8]H. P. Kuo and S. A. Korpela, "Stability and finite amplitude natural convection in a shallow cavity with insulated top and bottom and heated from a side," Phys. Fluids **31**, 33 (1988).
[9]T.-M. Wang and S. A. Korpela, "Convection rolls in a shallow cavity heated from the side," Phys. Fluids A **1**, 947 (1989).
[10]P. Laure, "Study of convective motions in a rectangular cavity with horizontal gradient of temperature," J. Theor. Appl. Mech. **6**, 351 (1987).
[11]P. Laure and B. Roux, "Linear and non-linear analysis of the hadley circulation," J. Cryst. Growth **97**, 226 (1989).
[12]M. G. Braunsfurth, A. C. Skeldon, A. Juel, T. Mullin, and D. S. Riley, "Free convection in liquid gallium," J. Fluid Mech. **342**, 295 (1997).
[13]A. Juel, J. Mullin, H. Ben Hadid, and D. Henry, "Three-dimensional free convection in molten gallium," J. Fluid Mech. **436**, 267 (2001).
[14]B. Hof, A. Juel, L. Zhao, D Henry, H. Ben Hadid, and T. Mullin, "On the onset of oscillatory convection in molten gallium," J. Fluid Mech. **515**, 391 (2004).
[15]W. Wang and R. X. Huang, "An experimental study on thermal circulation driven by horizontal differential heating," J. Fluid Mech. **540**, 49 (2005).
[16]G. O. Hughes and R. W. Griffiths, "Horizontal convection," Annu. Rev. Fluid Mech. **40**, 185 (2008).
[17]J. E. Weber, "On thermal convection between non-uniformly heated planes," Int. J. Heat Mass Transfer **16**, 961 (1973).
[18]D. Sweet, E. Jakeman, and D. T. J. Hurle, "Free convection in the presence of both vertical and horizontal temperature gradients," Phys. Fluids **20**, 1412 (1977).
[19]S. P. Bhattacharyya and S. Nador, "Stability of thermal convection between non-uniformly heated plates," Appl. Sci. Res. **32**, 555 (1976).
[20]J. E. Weber, "On the stability of thermally driven shear flow heated from below," J. Fluid Mech. **87**, 65 (1978).
[21]D. A. Nield, "Convection induced by an inclined temperature gradient in a shallow horizontal layer," Int. J. Heat Fluid Flow **15**, 157 (1994).
[22]P. N. Kaloni and N. Qiao, "On the nonlinear stability of thermally driven shear flow heated from below," Phys. Fluids, **8**, 639 (1996).
[23]M. Lappa, "Secondary and oscillatory gravitational instabilities in canonical three-dimensional models of crystal growth from the melt. ii: lateral heating and the Hadley circulation," C. R. Mec. **335**, 261 (2007).
[24]B. A. Finlayson, "The Galerkin method applied to convective instability problems," J. Fluid Mech. **17**, 201 (1968).
[25]B. A. Finlayson, *The Method of Weighted Residuals and Variational Principles*, Mathematics in Science and Engineering Vol. 87 (Academic, New York, 1972).
[26]W. H. Press, S. A. Teukolsky, W. T. Vetteling, and B. P. Flannery, *Numerical Recipes. The Art of Scientific Computing*, 3rd ed. (Cambridge University Press, Cambridge, 2007).
[27]S. Kaddeche, D. Henry, and H. Ben Hadid, "Magnetic stabilization of the buoyant convection between infinite horizontal walls with a horizontal temperature gradient," J. Fluid Mech. **480**, 185 (2003).
[28]W. M. Kays, *Convective Heat and Mass Transfer* (McGraw-Hill, New York, 1980), Appendix A, pp. 387–400.
[29]F. P. Incropera and D. P. DeWitt, *Fundamentals of Heat and Mass Transfer*, 3rd ed. (John Wiley and Sons, Inc., New York, 1990), Appendix A, page A24.
[30]J. P. Boyd, *Chebyshev & Fourier Spectral Methods*, Lectures Notes in Engineering Vol. 49 (Springer-Verlag, Berlin, Germany, 1989).